

## Microplastics Detection in Freshwater Lakes Using Sentinel-1 Synthetic Aperture Radar Images

Agilan B.<sup>1\*</sup>, Mithulesh P.<sup>1</sup>, Sourav Kumar N.R.S.<sup>1</sup> and Dr Vani K.<sup>1</sup>

<sup>1</sup>Department of Information Science and Technology, College of Engineering, Guindy, Chennai, India

[\\*agilan20042003@gmail.com](mailto:*agilan20042003@gmail.com)

**Abstract:** Microplastics in water bodies pose menacing threats to both aquatic ecosystems and human health once they infiltrate the food chain, it is imperative to devise an efficient methodology for detecting microplastics in water. This research endeavours to address a systematic approach to identify microplastics in inland water bodies using satellite imagery paired with deep learning. In-situ data mandatory for the study are mustered from open-source platforms like springeropen, containing coordinates of several water bodies and sampled data from particular dates. The pertinent Sentinel-1 Synthetic Aperture Radar data for dates mentioned in in-situ data are gathered. Obtained images are subjected to Lee's filter to handle the speckle noise present in them. In due course, a comprehensive dataset containing Vertical-Vertical + Vertical-Horizontal dual-polarisation data from Synthetic Aperture Radar images merged with corresponding in-situ data is created. The amalgamated dataset is utilised for training a multilayer perceptron model where the optimal hyperparameters are ascertained through executing Optuna, a hyperparameter optimization framework. Additionally, K-fold cross-validation is employed to assess the model performance in a robust manner exploring different subsets of the merged dataset. The trained multilayer perceptron model with the best possible hyperparameters scores a commendable R-squared value of 0.85, subsequently, the trained model is engaged in the production of inversion images for any designated target water body for whom Sentinel-1 Synthetic Aperture Radar images are obtainable representing the concentration of microplastics in them. Henceforth this study provides a formidable methodology for evaluating the existence and density of microplastic particles within inland water bodies safeguarding public health and paving the way for a sustainable environment.

**Keywords:** Deep learning, Microplastics, Multilayer perceptron, Synthetic Aperture Radar.

### Introduction

Microplastics (MP) present in inland water bodies have emerged as a significant contaminant, impacting the health of aquatic ecosystems and the public who rely on these water sources. The demand for plastics is growing across the world since they are widely used for commercial, and medical industries serving various purposes including packaging, medical instruments, construction and so on. These plastics used for a short duration are disposed of quickly. These disposed plastics degrade over time resulting in

the breaking down of polymers within them ultimately causing them to break into tiny pieces. These degraded plastics ranging in size from 1  $\mu\text{m}$  to 5 mm in diameter are referred to as MPs. The discharge of MPs occurs through various sources, including run-off from contaminated land, municipal wastewater or atmosphere deposition. Their presence can cause genetic damage to aquatic species and health problems for humans relying on inland water sources for drinking purposes. Hence it is essential to detect the presence and volume of MPs present in the inland water bodies and assess their suitability for use as drinking water.

### **Literature Review**

The global demand for plastics keeps on increasing due to their versatile usage across many industries and household activities. The extensive use of disposable plastic packaging makes waste management challenging. They tend to stay in the environment for a long period and affect the ecosystem. A certain amount of these plastics is degraded to microplastics (Thompson et al., 2004) by the effect of Ultraviolet (UV) exposure, temperature and biological degradation (Ali Chamas et al., 2020). Jaswant Singh et al. (2024) studied the contamination of water bodies, including lakes, rivers, and ponds, by microplastics in India. It provided a perspective on the sources, composition and distribution of them. The collected sample underwent various pre-treatment processes including digestion and density separation using chemicals like Zinc Chloride ( $\text{ZnCl}_2$ ) and Sodium chloride (NaCl) to isolate MPs from other materials. Post-purification, fluorescent microscopy was initially used to identify the MPs followed by confirmation through Fourier Transform Infrared Spectroscopy (FTIR). This approach is better suited for analysing the physical and chemical properties of the Microplastics present in the water bodies. The study also highlights the significant variability in methodologies used for sampling, processing, and analysing MPs. It also acknowledges that on-site measurements are time-consuming and do not capture the temporal variability.

This challenge can be overcome by utilising remote sensing to detect the presence of MPs. Ahmed Mohsen et al. (2023) conducted a study on the quantification of the MPs present in the Tisza River in Central Europe by analysing the relationship between the concentration of MPs and their reflectance/backscattering of various passive and active space-borne sensors. This study utilised data from the Sentinel-2, PlanetScope, and Sentinel-1 sensors to analyse the concentration of MPs in water bodies.

Another study carried out by Morgan David Simpson et al. (2022) found that Sentinel-1 Synthetic Aperture Radar (SAR) data is more suitable for assessing the plastic accumulation in rivers compared to Sentinel-2 optical imagery since it provides fine spatial resolution imaging that can be monitored in all light and weather conditions. Sentinel-2 optical imagery faces limitations due to its coarse resolution and unavailability of the data due to cloud cover and weather conditions. However, this study is limited by the number of samples collected from the target site which can possibly affect the accuracy of the analysis.

Abhinav Verma et al. (2024) assessed the spatial variations in scattering power by different land covers using the Ground Range Detected (GRD) dual-polarisation SAR data from Sentinel-1 Mission. GRD data captures well the scattering information of the particles from the dual-pol SAR data. The methodology employed in this study guaranteed the preservation of the total scattered power from the SAR data.

However, this Sentinel-1 is affected by speckle noises due to the interference of the radar signals scattered resulting in constructive and destructive patterns (Alessandro Sebastianelli et al. 2022). It causes variation in pixel intensity thus creating a granular appearance in the image. The removal of the speckle noise can be efficiently done using Refined Lee Filter as suggested by Aiyeola Sikiru Yommy et al. (2015). RLF is an enhancement to the original Lee Filter by employing the K-Nearest Neighbour (KNN) algorithm. It is also found to be superior for filtering the speckles of the SAR images.

Marius-Constantin Popescu et al. (2009) suggested using Multilayer perceptron (MLP) a Deep Learning (DL) model for solving complex, non-linear problems by minimising the difference between the desired and the actual output through the downward gradient method. MLPs can handle a wide range of data types and are effective in recognising patterns in data. They involve defining a set of hyperparameters to identify the patterns.

Finding the right hyperparameters in any DL model is often a resource-intensive task. With the increasing trend in DL, an optimal way of finding the better-performing hyperparameter is the need of the hour. Takuya Akiba et al (2019) proposed Optuna, a next-generation hyperparameter optimization framework. It works by a technique called define-by-run where there is no need to explicitly define the hyperparameters in prior. Optuna optimises the hyperparameter space by minimising or maximising an objective function whose input will be a combination of hyperparameters and returns the assessment

score of that combination. The objective function is gradually built through interaction with trial objects with dynamic construction of search spaces of the trial object. Optuna creates an effective pruning algorithm by using a modified version of Asynchronous Successive Halving (ASHA), where an early worker can aggressively stop trials asynchronously based on their provisional ranking. The efficiency of the Optuna framework became prominent when it became the key player in Preferred Networks' Faster Region-based Convolutional Neural Network (R-CNN) models, High-Performance Linpack (HPL), RocksDB and more.

The challenges posed by these studies including time-consuming in situ measurements, lack of data samples for the analysis, using speckled data for analysis and not using the full potential of Sentinel-1 SAR data are addressed by utilising Vertical-Vertical + Vertical-Horizontal (VV + VH) bands of the SAR data which offer polarisation diversity and is used to detect the MPs by analysing their orientation in the water bodies. Also, the diverse nature of the dataset considered in this study proved to be effective for better results. Also, the despeckling of the SAR data before analysis enhanced the accuracy of the result.

## **Methodology**

In this section, the step-by-step processes involved in Microplastics detection are explained, as depicted in Figure 1 for better understanding and reference throughout the study.

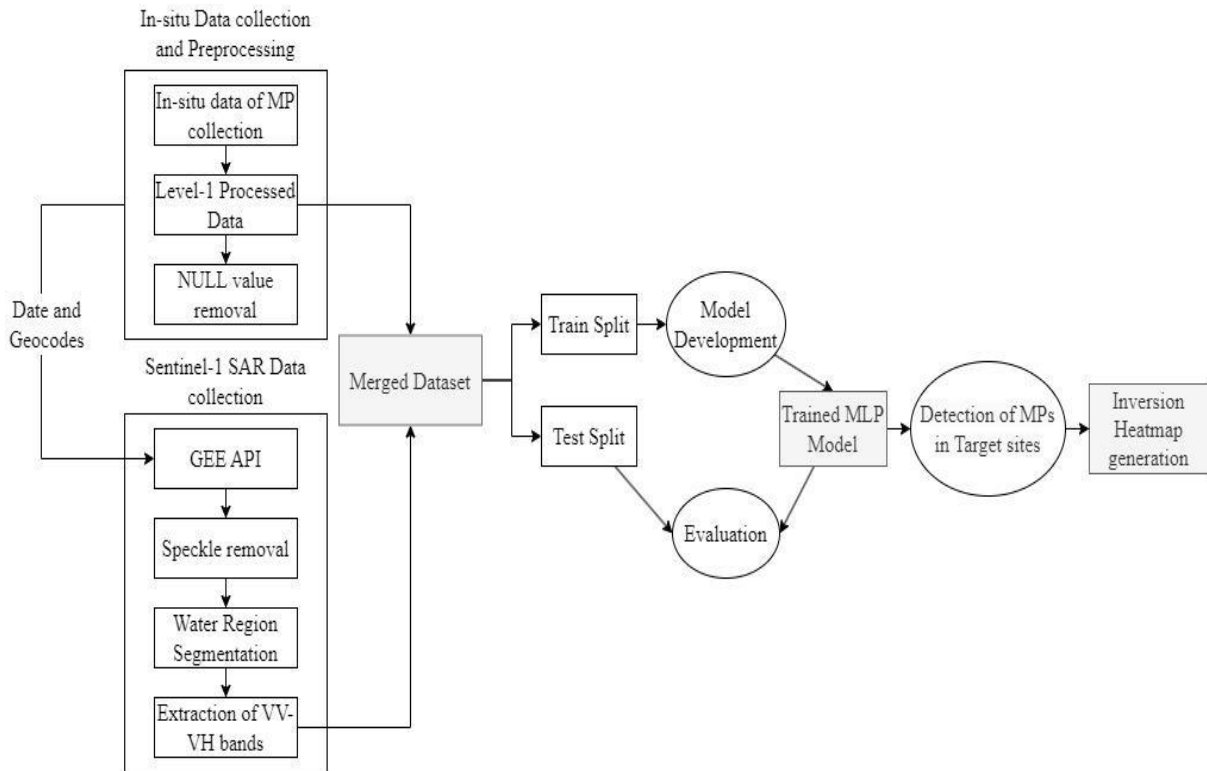


Figure 1: Overall architecture of the study

**Data Collection:** A total of 8,218 samples of MPs were collected by Atsuhiko Isobe et al. (2021) from global oceans and freshwater bodies over a period of 19 years from 2001 to 2019. It was used to create a dataset and was made available to the public. This dataset includes the date and coordinates of each sample collected as well as the raw data and various levels of processed data: level 1 (processed by removing fibrous MPs), level 2p (processed for wind/wave correction), level 2w, level 3p, and level 3w. Our study considered the level 1 processed data for analysis since it constituted MPs with sizes that are less than 5mm in size. The unit of the processed and calibrated data is particles/L. Additionally, the dataset includes samples with no trace of MPs which will help the model understand better the relationship between microplastics and their backscattering effects. Finally, the corresponding Sentinel-1 SAR GRD of the water samples were collected from the Google Earth Engine (GEE) Application Programming Interface (API) by inputting the Date and location of the analysis. These SAR data can overcome the presence of clouds by penetrating through them and capturing the data regardless of the weather conditions during the sampling of the MPs. Hence this data is found to be superior to that of the Sentinel-2 and Landsat-8 data whose data will be affected by the presence of the cloud cover and weather conditions. The SAR data consisted of four bands: Horizontal transmit/Horizontal receive (HH), Horizontal transmit/Vertical receive (HV), Vertical

transmit/Vertical receive (VV) and Vertical transmit/Horizontal receive (VH). Once the in-situ data and SAR data are collected they are subjected to further processing for better analysis of the results.

**Data Preprocessing and Dataset Creation:** First, the in-situ dataset was pre-processed to contain only the date, geolocations and level 1 processed data of the MPs. Since the SAR data was available only from Oct 2014, any samples collected before that are removed from the dataset to avoid unnecessary interference. It also ensured that the pre-processed dataset was free of null values and outliers. Next, GEE API is used to collect SAR data from the Sentinel-1 mission. It consists of S1 GRD scenes processed using the Sentinel-1 toolbox to produce calibrated and ortho-corrected products. Date and geocodes are specified along with a buffer radius of 10 metre around the location. The collected data is filtered for VH polarisation in Interferometric Wide (IW) mode. We then particularly select VV and VH bands and export the data to Google Drive. The specifications of the Sentinel-1 SAR data used for this study are outlined in Table 1.

Table 1: Specification of Sentinel-1 image

Property	Sentinel-1
Sensor Type	Synthetic Aperture Radar (SAR)
Frequency	C-band (5.405GHz)
Data Type	GRD scenes
Resolutions	10, 25, or 40 metres
Band Combinations	Single band VV or HH Dual-band VV+VH or HH+HV
Instrument Modes	3 modes

The collected data are downloaded from the cloud and subjected to filtering to remove the speckles. Speckle noises arise due to the coherent nature of the radar signal. It is caused by the constructive and destructive interference of the radar waves scattered by the particles within a single-resolution cell. This interference results in a granular, salt and pepper noise pattern in the radar image. The presence of these noises can obscure the Image Quality and make the analysis complicated and inaccurate. Hence for removing them, the Lee filter is used while preserving the important image features. This filter operates by computing the mean and variance of the neighbouring pixels present within a local window for each pixel at its centre. Additionally, the KNN algorithm is employed as suggested by Aiyeola Sikiru Yommy et al. (2015) to create a refined Lee Filter by modifying the number of neighbouring pixels within the considered sliding window. Then it uses local statistics to estimate the weighing factor. This factor determines how much the pixel value should be smoothed based on the ratio of the local to overall variance. Hence the resulting image is free of speckles in addition to preserving edges and important features in it.

Once the speckles are removed, the images are subjected to water region segmentation by removing the land area of the water body from interfering with the estimation of the MP concentration. We apply a threshold on the dual polarisation values to classify the pixels for the presence of water bodies and land regions. Any pixel with value less than this threshold will be classified as water body and those with greater than the threshold will be classified as land region. The water mask is created and applied to the original data to nullify the land area present in it.

We then extract the VV + VH dual polarisation bands present in the filtered, water-segmented image due to its increased sensitivity to different surfaces and subsurface characteristics. Finally, it is merged with the dataset containing the level 1 processed data of MP samples. Thus, the final merged dataset contains the volume of MPs and their values of backscattering power received by the sensor. This dataset better captures the relationship since it includes samples with 0 volumes of MPs. This dataset is used for the training of the models to better understand their relationship.

**Model Development and Evaluation:** Once the final dataset is created, it is used to train the Multilayer perceptron (MLP) model, a supervised Feed-forward Neural Network (FNN). It consists of multiple layers including input, hidden and output layers where each layer contains fully connected neurons called perceptrons. The hidden and output layers employ a nonlinear activation function. This neural network contains many hyperparameters including the size of the hidden layers, activation function, optimization algorithm, Regularisation term also known as Alpha to prevent overfitting, Learning rate, maximum number of iterations for the training and size of mini-batches for stochastic optimizers. The objective before training the model is to search the hyperparameter space to find optimal parameters for more accurate results.

Hence, we leverage Optuna, a hyperparameter optimization algorithm that in turn leverages the Bayesian optimization techniques to efficiently find the best hyperparameter for training the MLP regressor model. The goal is to maximise the model performance by obtaining the best possible combination of the hyperparameters. First, the objective function is defined with the hyperparameters and all possible values of them. Optuna then creates a study and aims to optimise the objective over 1000 trials. In each trial, optuna calls this function with different combinations of the hyperparameters and trains and evaluates the MLPRegressor to find the best set. To compute the performance of each hyperparameter combination considered, k-fold cross-validation (CV) with  $K=5$  is used. This CV methodology divides the dataset into 5 equally sized folds. The model will be trained on the 4 folds (one fold less than the value of  $K$ ) and validated on the remaining one fold. This process is repeated four times, with each iteration using a different fold as the validation set. The Coefficient of determination ( $R$ -squared/ $R^2$ ) and the Root Mean Square Error (RMSE) are computed during each step and their means are returned. This type of evaluation ensures that the performance of the model is robust and does not depend much on any single subset of the data split by the CV methodology. At the end of



all the trials, the best hyperparameters which tend to maximise the  $R^2$  score and minimise the RMSE are found. The equations for RMSE and  $R^2$  are defined as follows.

The  $R^2$  score is given by:

$$R^2 = 1 - \frac{\sum_{i=1}^n (y_i - \hat{y}_i)^2}{\sum_{i=1}^n (y_i - \bar{y})^2}$$

Whereas RMSE is given by,

$$RMSE = \sqrt{\frac{1}{n} \sum_{i=1}^n (y_i - \hat{y}_i)^2}$$

**Detection of Microplastics:** Finally, the model is defined with the best set of hyperparameters. The dataset is split into train and test sets. The model defined will validate the train set using K-fold CV to capture every pattern available. The  $R^2$  score for each fold is estimated and averaged to yield the overall accuracy of the model over the train set. The trained model is validated against the test set. Now the model is set up to predict the concentration of MPs for the test site provided, we start inputting the Satellite (SAR) data of that location and generate inversion heat maps of it.

**Inversion Heatmap generation:** After the model has been trained, we can proceed with the prediction of the volume of MPs present in a water body. First, we obtain the date and location of the site to be investigated. This is inputted into the GEE API for obtaining the corresponding Sentinel-1 SAR GRD data. The obtained image is corrupted with speckles due to interference which will be removed by the same methodology followed during data preprocessing for training with the help of Refined Lee Filter. Thus, the obtained image will be free of speckles and used for the prediction. The filtered image is subjected to water region segmentation to neglect the effect of the land areas on the analysis. The VV and VH bands are extracted for each pixel of the SAR image and provided as input for the trained MLP regression model to output the volume of the microplastics present in each pixel. The predicted values are used to generate an inversion heat map depicting the target site to be presented for the analysis. These values are averaged to obtain the mean volume of MPs present in the water body.

There are no standards yet to classify the water body if it is suitable for drinking water. The World Health Organization (WHO) declared that in the studies on freshwater, the volume of MPs reported ranged from 0 to 10000 particles/L. However, nine studies reported that the particle count in drinking water ranged with a mean value from  $10^{-3}$  to

1000 particles/L. However, there is no study yet defining the permissible volume of MPs that can be present in the water that would not impact its safety for drinking. Hence it can be assumed that water sources containing MPs with a mean volume between  $10^{-3}$  to 1000 particles/L can be suggested for drinking purposes.

## Results and Discussion

Initially, the dataset was collected from the open-source website published by Atsuhiko Isobe et al. (2021). It consisted of 8,218 samples from 2001 to 2019. All the samples collected before Oct 2014 are removed. After removing the null values and outliers the resulting dataset consisted of 171 rows with features Date, geocodes and level 1 processed data of MPs concentration in particles/L.

Next, the Sentinel-1 SAR data are collected from the GEE API for the dates and geocodes corresponding to the pre-processed dataset. It contains VV and VH bands. This extracted image contains speckle noises due to the interference and it is removed by applying the Refined Lee Filter to it. The figures 2 and 3 present the image before and after removing the speckle noises from the SAR data of Puzhal and Veeranam Lakes respectively.

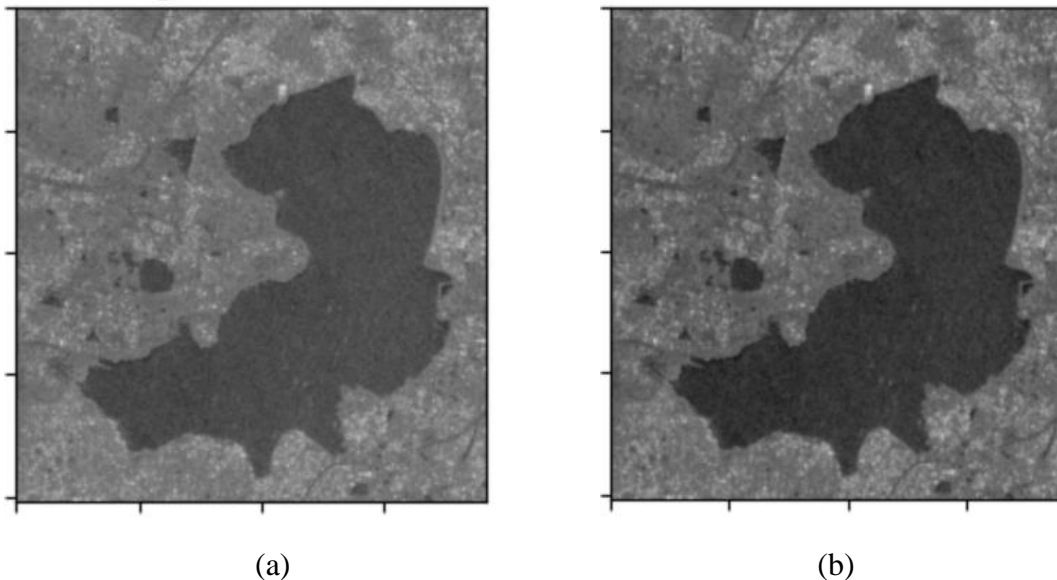


Figure 2: Sentinel-1 SAR data of Puzhal before and after speckle filtering

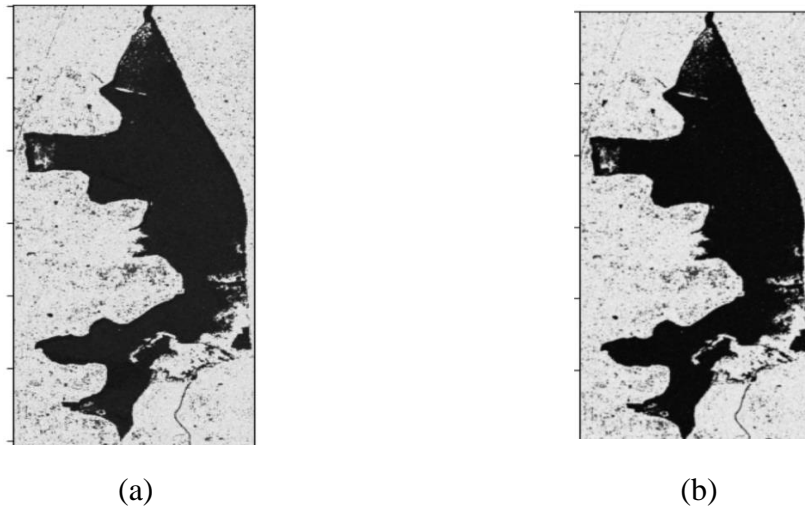


Figure 3: Sentinel-1 SAR data of Veeranam before and after speckle filtering

After removing the speckles, the water region present is segmented by applying a threshold value to the VV and VH bands. The pixels with values of VV and VH less than a threshold value of -12.5 will be considered as water pixels while those with value greater than -12.5 will be considered to contain land regions. This enables us to create a water mask with the True values for water pixels and False values for non-water pixels. This water mask will be applied over the original image to obtain a water-segmented image. The figures 5 and 6 present the SAR data before and after removing the land region from it by thresholding of the two lakes.

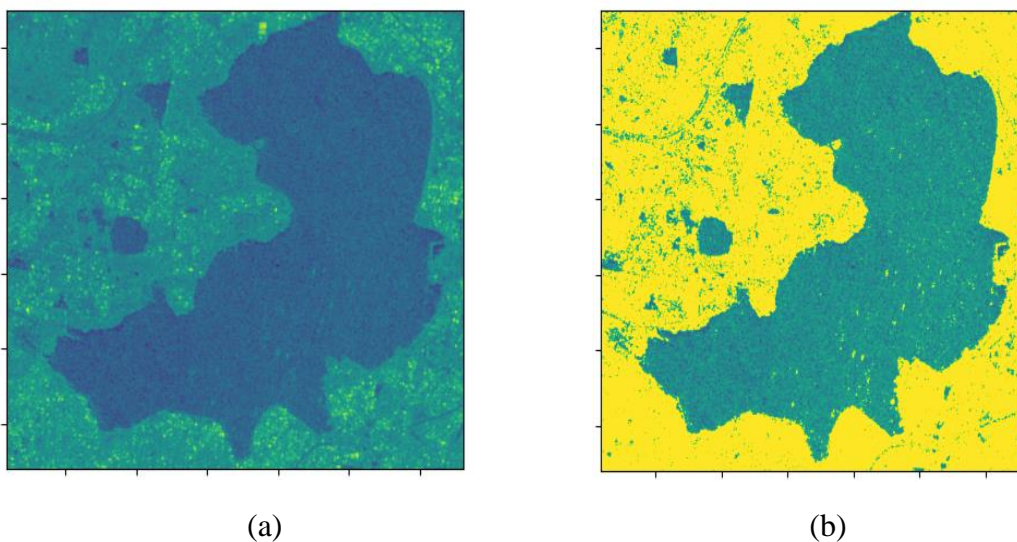


Figure 6: Sentinel-1 SAR data of Puzhal before and after water segmentation

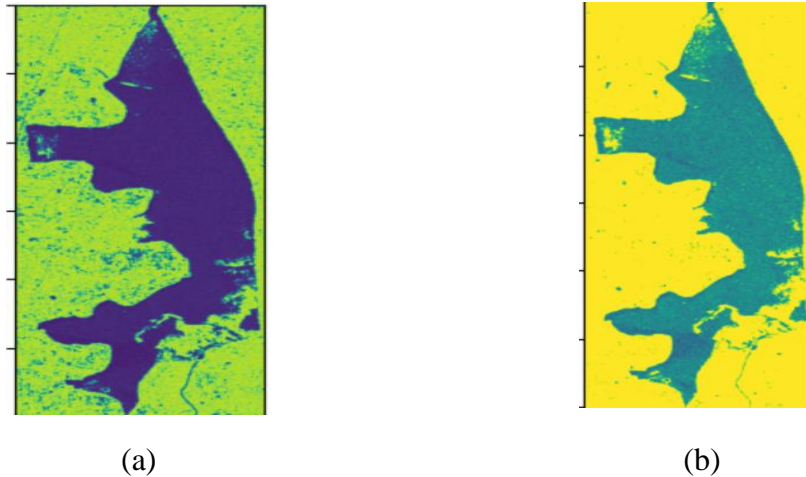


Figure 5: Sentinel-1 SAR data of Veeranam before and after water segmentation

After these steps, the VV and VH bands are extracted from the final image and merged with the Level 1 processed data containing the volume of the MPs. The figure 6 presents a subset of the finally merged dataset for model training.

MP	Sigma0_VH_db	Sigma0_VV_db
0.709	-47.76744271	-17.02674612
0.955	-42.61007307	-20.60221869
1.1	-33.13300388	-20.10734355
1.11	-39.08020158	-17.62141114
0.975	-31.21274452	-20.35073394
0.887	-38.35491116	-26.24421206
0.757	-44.04265106	-29.50364611
1.06	-42.29689608	-20.06006044
1.29	-42.50385273	-20.43247245
1.14	-45.68156439	-24.44755877
1.23	-46.72965756	-33.34844081
1.13	-45.02341425	-21.76335286
1.5	-32.88376667	-22.39056793
3.09	-31.44344155	-12.95310489
0.153	-39.0777167	-14.86703704
0	-38.76167808	-18.82779501
0.106	-37.21045725	-22.0942198
1.06	-37.19777389	-24.1454413
0.0502	-36.1341039	-22.25010013

Figure 6: Final merged dataset for model training

The correlation between MP and the scattering power is analysed and outlined as a heatmap in Figure 7.

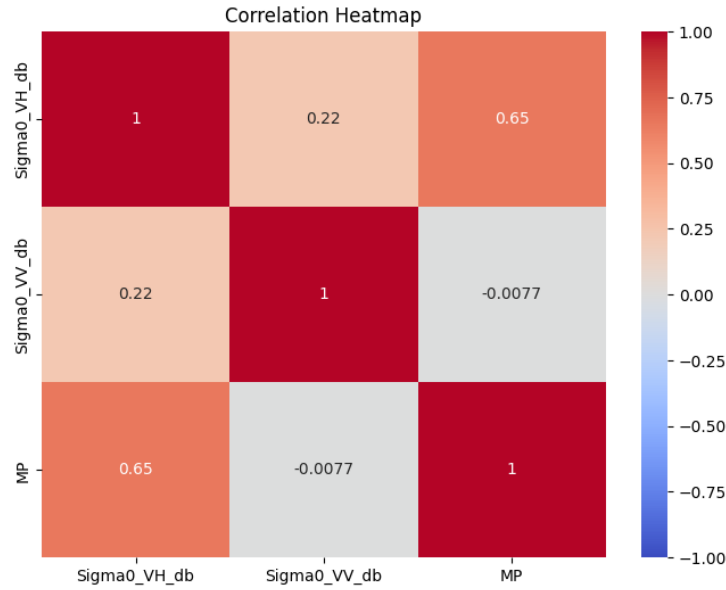


Figure 7: Correlation between the volume of MPs and backscattering power

After creating the final merged dataset, the training of the MLP model is carried out with it. Before training the model, the hyperparameters used for defining the model need to be identified. Opunta is used for searching the hyperparameter space to identify the best combination of the hyperparameters yielding more accurate results. Opunta works by defining an objective function containing all possible values of the hyperparameter space and runs about 1000 trials to locate the best possible combination. Figure 8 presents the mechanism of working of Opunta.

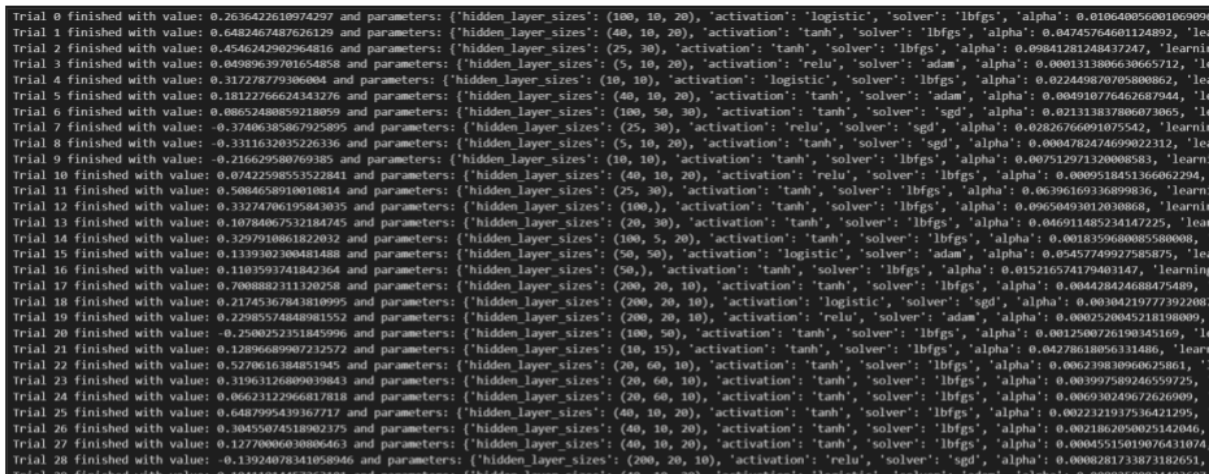


Figure 8: Hyperparameter optimization using Optuna

The list of hyperparameters of the MLP model, their possible values and the best value chosen is outlined in table 2 below.

Table 2: List of hyperparameters, possible values and the best values chosen

Hyperparameter	All possible values	Best Hyperparameter
Size of hidden layers	(50,), (100,), (50,50), (100,50), (20,60,10), (5,10,20), (100, 5, 20), (100, 10, 20), (10, 10), (10, 15), (20,30), (25, 30), (40, 10, 20), (100, 50, 30), (200, 20, 10)	(100, 50)
Activation functions	relu, tanh, logistic	logistic
Optimization algorithm	lbfgs, sgd, adam	lbfgs
Alpha	1e-4, 1e-1	1.67e-4
Learning Rate	constant, invscaling, adaptive	adaptive
Maximum number of iterations	100 to 1000	375
Batch Size	32 to 128	34

After obtaining these hyperparameters the dataset is split into train and test sets with 80:20 ratio. The model is trained with these hyperparameters on the train set using K-fold cross-validation with K=5. The  $R^2$  and RMSE scores obtained from each fold are listed in Table 3.

 Table 3: Values of  $R^2$  and RMSE resulting from each fold of the train set

Fold No.	$R^2$	RMSE
1	0.87	2.96
2	0.62	11.51
3	0.69	6.48
4	0.89	2.66
5	0.90	1.75

The mean of the  $R^2$  is calculated to establish the overall accuracy of the model on the train set. The trained model provided a mean  $R^2$  score of 0.79. Figure 9 presents the  $R^2$  scores of each fold obtained.

After this, the model is used to validate the test set which yielded an  $R^2$  score of 0.85.

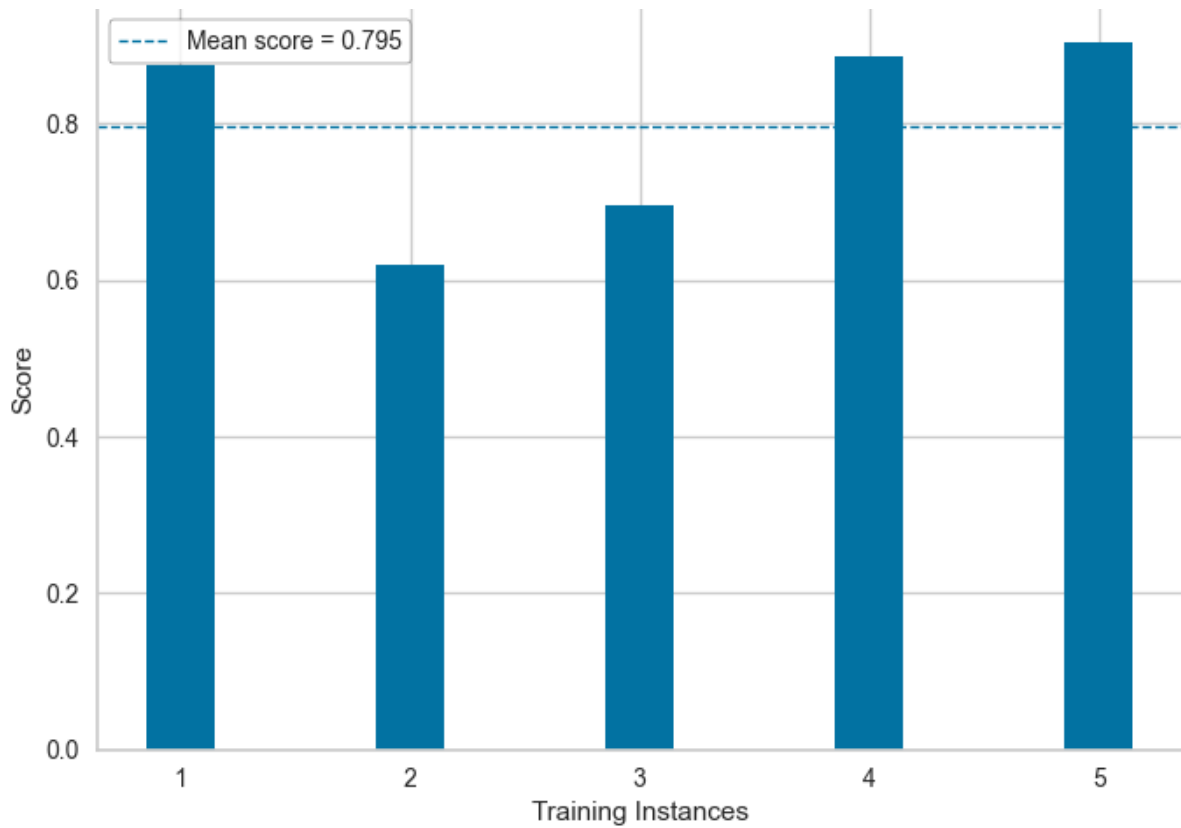


Figure 9: Cross-validation scores for MLPRegressor

Once the training of the model is completed, we can proceed with predicting the volumes for any target site. First, the geolocations of the target site and the date on which the prediction is to happen are inputted into the GEE API and corresponding SAR data is obtained. Here we considered the data of Lake Veeranam in Tamil Nadu for this analysis. We then subject it to speckle filtering and water region extraction before providing its value to the model. The VV and VH dual-pol values of each pixel are provided as input to the model and the volume of MP is produced as output. The MP value of all pixels is used to generate an inversion heatmap. Figures 10 and 11 present the Sentinel-1 data and the resulting inversion heatmaps of the target lakes, Puzhal and Veeranam.



Figure 10: Detection of microplastics in Puzhal

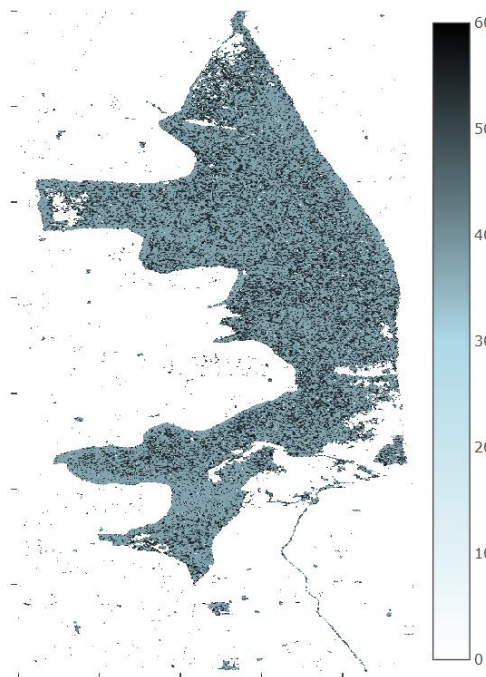


Figure 11: Detection of microplastics in Veeranam

The average predicted values are 8.65 and 43.64 particles/L respectively. Veeranam Lake showed significantly high levels of MPs, while Puzhal has comparatively low levels. Figure 12 presents the declaration of the reported concentration of microplastics in freshwater and drinking water sources by WHO. From this report, we can conclude that



there are no standards yet defined for the permissible amounts of MPs that do not affect the safety level of drinking water.

### How much microplastic has been found in drinking-water and drinking-water sources?

In freshwater studies, reported microplastic particle counts ranged from around 0 to 1000 particles/L. Only nine studies were identified that measured microplastics in drinking-water; these studies reported particle counts in individual samples from 0 to 10 000 particles/L and mean values from  $10^{-3}$  to 1000 particles/L. A comparison of the data between fresh water and drinking-water studies should not be made because in most cases freshwater studies targeted larger particles, using filter sizes that were an order of magnitude larger than those used in drinking-water studies.

Figure 12: Report of WHO about Microplastics in freshwater and drinking water

## Conclusion and Recommendation

For mitigation of environmental and health risks, associated with these pervasive pollutants, the detection of microplastics in freshwater lakes from Sentinel-1 SAR imagery is a solution using DL techniques. This paper fuses the high spatial resolution of SAR with a trained MLP model on a large dataset of SAR-derived backscattering and in-situ measured microplastic concentrations.

This approach will help overcome some of the limitations of traditional optical sensors through the use of Sentinel-1 SAR data, which easily penetrates through clouds and efficiently works in any climatic condition. First, pre-processing is done on SAR images to remove speckle noise, followed by the segmentation of water bodies into separate areas contaminated with microplastics. The MLP model optimises the Optuna framework for hyperparameter tuning and makes a robust prediction of microplastic concentration validated with an R-squared score of 0.85.

Spatial insights into the microplastic distribution within water bodies that are obtained by inversion heatmaps from the model output can help devise a targeted pollution management strategy. The setting of standardised regulations on microplastic levels in drinking water and the increase of datasets across the broadest geographical regions as research progresses will further increase the applicability and impact of SAR-based microplastic detection methods. An integrated approach such as this will move scientific

understanding forward in support of sustainable water resources management and environmental stewardship.

## References

Aiyeola Sikiru Yommy, Liu, R., & And Shuang Wu. (2015). *SAR Image Despeckling Using Refined Lee Filter*. <https://doi.org/10.1109/ihmsc.2015.236>

Akiba, T., Sano, S., Yanase, T., Ohta, T., & Koyama, M. (2019). Optuna: A Next-generation Hyperparameter Optimization Framework. *arXiv (Cornell University)*. <https://doi.org/10.48550/arxiv.1907.10902>

Chamas, A., Moon, H., Zheng, J., Qiu, Y., Tabassum, T., Jang, J. H., Abu-Omar, M., Scott, S. L., & Suh, S. (2020). Degradation rates of plastics in the environment. *ACS Sustainable Chemistry & Engineering*, 8(9), 3494–3511. <https://doi.org/10.1021/acssuschemeng.9b0663>

Isobe, A., Azuma, T., Cordova, M. R., Cózar, A., Galgani, F., Hagita, R., Kanhai, L. D., Imai, K., Iwasaki, S., Kako, S., Kozlovskii, N., Lusher, A. L., Mason, S. A., Michida, Y., Mituhasi, T., Morii, Y., Mukai, T., Popova, A., Shimizu, K., & Tokai, T. (2021). A multilevel dataset of microplastic abundance in the world's upper ocean and the Laurentian Great Lakes. *Microplastics and Nanoplastics*, 1(1). <https://doi.org/10.1186/s43591-021-00013-z>

Mohsen, A., Kovács, F., & Kiss, T. (2023). Riverine Microplastic Quantification: A Novel Approach Integrating Satellite Images, Neural Network, and Suspended Sediment Data as a Proxy. *Sensors*, 23(23), 9505. <https://doi.org/10.3390/s23239505>

Morgan David Simpson, Marino, A., Peter de Maagt, Gandini, E., Hunter, P., Evangelos Spyarakos, Tyler, A., & Telfer, T. (2022). Monitoring of Plastic Islands in River Environment Using Sentinel-1 SAR Data. *Remote Sensing*, 14(18), 4473–4473. <https://doi.org/10.3390/rs14184473>

Popescu, M.-C., Balas, V., Perescu-Popescu, L., & Mastorakis, N. (2009). Multilayer perceptron and neural networks. *WSEAS Transactions on Circuits and Systems*, 8, 579–588.

[https://www.researchgate.net/publication/228340819\\_Multilayer\\_perceptron\\_and\\_neural\\_networks](https://www.researchgate.net/publication/228340819_Multilayer_perceptron_and_neural_networks)

Sebastianelli, A., Pia, M., Ullo, S. L., & Gamba, P. (2022). A Speckle Filter for Sentinel-1 SAR Ground Range Detected Data Based on Residual Convolutional Neural Networks. *IEEE Journal of Selected Topics in Applied Earth Observations and Remote Sensing*, *15*, 5086–5101. <https://doi.org/10.1109/jstars.2022.3184355>

Singh, J., Yadav, B. K., Schneidewind, U., & Krause, S. (2024). Microplastics pollution in inland aquatic ecosystems of india with a global perspective on sources, composition, and spatial distribution. *Journal of Hydrology. Regional Studies*, *53*, 101798–101798. <https://doi.org/10.1016/j.ejrh.2024.101798>

Thompson, R. C. (2004). Lost at Sea: Where Is All the Plastic? *Science*, *304*(5672), 838–838. <https://doi.org/10.1126/science.1094559>

Verma, A., Bhattacharya, A., Dey, S., López-Martínez, C., & Gamba, P. (2024). Scattering power components from dual-pol Sentinel-1 SLC and GRD SAR data. *ISPRS Journal of Photogrammetry and Remote Sensing*, *212*, 289–305. <https://doi.org/10.1016/j.isprsjprs.2024.05.010>